Superficies y Vacío ***26(3)*** *107-110, septiembre de 2013*

Study of $In_xGa_{1-x}N$ layers growth on GaN/Al_2O_3 by MOCVD at different pressures

Guarneros C. * Espinosa J. E.
Posgrado en Física Aplicada, Facultad de Ciencias Físico-Matemáticas
Benemérita Universidad Autónoma de Puebla
Blvd. 14 Sur 6301, Col. San Manuel, 72570, Puebla, México

Sánchez V. M.
Sección de Electrónica del Estado Sólido, Departamento de Ingeniería Eléctrica
Centro de Investigación y de Estudios Avanzados del Instituto Politécnico Nacional
Av. I. P. N. 2508, San Pedro Zacatenco, 07360, México, D. F.

López U.
Facultad de Ingeniería Química, Benemérita Universidad Autónoma de Puebla
Blvd. 14 Sur 6301, Col. San Manuel, 72570, Puebla, México.
(Recibido: 14 de noviembre de 2012; Aceptado: 26 de agosto de 2013)

We present the $In_xGa_{1-x}N$ layers growth in a metalorganic chemical vapor deposition (MOCVD) system. First, we growth a GaN epitaxial layer on sapphire substrate, trimethylgallium (TMGa) and ammonia (NH_3) are precursors of gallium and nitrogen, respectively, and hydrogen (H_2) is used as the carrier gas. Later, on the GaN epilayer, the growth of the $In_xGa_{1-x}N$ layer is carried out using trimethylindium (TMIn) as the indium precursor. The $In_xGa_{1-x}N$ layers were studied using X-ray diffraction (XRD) and scanning electron microscopy (SEM). XRD pattern shows the diffraction lines which could be ascribed to the formation of hexagonal $In_{0.115}Ga_{0.885}N$ for sample A, and $In_{0.26}Ga_{0.74}N$ for sample B, both with the wurtzite type structure. SEM images illustrate the effect of the growth pressure on the films surface morphology. At low pressure the sample A has smaller grain size and higher nuclei density; at high pressure the island size increases and has lower density (sample B). The alloy formation is favored at 550 Torr.

Keywords: $In_xGa_{1-x}N$ alloys; Growth pressure; XRD patterns; Indium concentration; Vegard's law

1. Introduction

$In_xGa_{1-x}N$ alloys are potential materials for the fabrication of blue/green light emitting diodes LEDs, and violet/blue injection lasers LDs, since the band gap energy of $In_xGa_{1-x}N$ can be varied from 3.4 to 0.7 eV by increasing the InN concentration and the potential operating wavelengths cover nearly the entire visible spectral range. However, the growth of $In_xGa_{1-x}N$ alloys using MOCVD has proven to be extremely challenging, mostly due to the trade-off between the epilayer quality and the amount of InN incorporation into the alloy as the growth temperature is changed. The low solubility of InN in GaN and the large solid phase miscibility gap phase separation and compositional inhomogeneity are commonly observed in $In_xGa_{1-x}N$ alloys, which may have both advantageous and detrimental effects upon the performances of the devices. Experimental observations of splitting double X-ray diffraction peaks in InGaN alloys are used to be considered as the evidence of compositional inhomogeneity [1].

According to X. L. Zhu *et al.* multiple diffraction peaks are observed in X-ray diffraction from InGaN layers and some caution is required when interpreting the peaks, especially a diffraction peak at about $2\theta \approx 33°$, which may originate from different possible causes. The two main points of view consider the peak related to phase separation of about 50% InGaN in the InGaN alloy matrix evidenced by XRD and metallic indium nanowires in an InGaN matrix analysis. Indium penetrates through InGaN film with small lateral size of nanometers with its (101) plane parallel to (0001) InGaN surface [2, 3].

On the other hand, the indium incorporation increase significantly as the growth temperature decreased. In order to investigate the pressure effects on $In_xGa_{1-x}N$ layer growth we carried out experiments with two different pressures, at 50 Torr and 550 Torr.

2. Methodology

$In_xGa_{1-x}N$ layer was grown by MOCVD horizontal quartz reactor. The precursors were trimethylgallium, trimethylindium and ammonia for Ga, In, and N, respectively. The ~1 μ thick GaN templates were grown on (0001) oriented (Al_2O_3) sapphire substrates at 900° C prior to the growth of $In_xGa_{1-x}N$ layers, the experimental details are given in references [4, 5]. Two different samples were grown at low temperature (600° C), the sample A was grown at 50 Torr and the sample B was grown at 550 Torr, during 30 minutes, respectively. TMGa flow rates were A) 4.4 μmole/min, B) 7.19 μmole/min, and TMIn flow rate for the two samples was 3.14 μmole/min. Ammonia flow rate was 0.5 slm, and H_2 flow rate was 3.5 slm for both samples. The $In_xGa_{1-x}N$ layers were studied using XRD and the surface morphology was studied by SEM. The indium concentration in the layers was determined from XRD

*cesyga@yahoo.com.mx

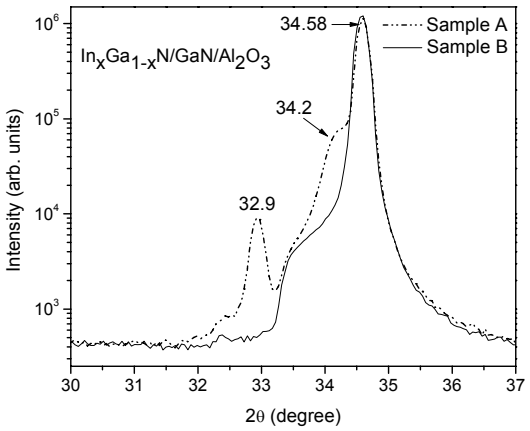

Figure 1. X-ray diffraction pattern of $In_xGa_{1-x}N$ layers growth on GaN/α-Al_2O_3. The peaks at 34.58°, 34.2°, and 32.9°, represent the (0002) diffraction peak of GaN with wurtzite structure, InN diffraction peak and indium diffraction peak, respectively, for sample A. The x-ray diffraction pattern for sample B shows the peak of GaN (0002) at 34.58° with a wide shoulder.

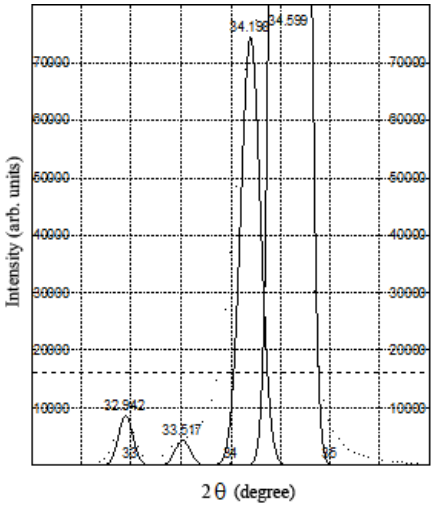

Figure 2. Deconvolution of X-ray diffraction pattern for sample A. The peaks at 34.59° and 33.51° represent the (0002) diffraction peaks of GaN with wurtzite structure and In_xGa_{1-x} (0002) diffraction peak, respectively. The peaks located at 34.2° and 32.94° correspond to InN (111) and In (101) diffraction peaks, respectively.

patterns and the band gap was calculates using the Vegard's law.

3. Results and Discussion

X-ray diffraction (XRD) measurements were performed using an X-Ray Diffractometer Panalytical X-Pert Pro MRD with Cu target operated at 40 kV and 20 mA. Figure 1 shows the X-ray diffraction pattern of $In_xGa_{1-x}N$ layers, A and B, grown on GaN/α-Al_2O_3 templates. However, multiple diffraction peaks are observed in this x-ray diffraction patterns. Many researchers have been studied the solid phase immiscibility in $In_xGa_{1-x}N$, which occurs due to large difference in interatomic spacing (with lattice mismatch ~11.25% between the two end binaries, GaN and InN). This immiscibility results in phase separation and growth instabilities in $In_xGa_{1-x}N$ system [6-9]. Thus, for the two samples synthesized, it can observe the presence of the GaN and InN phases. For the sample A, the XRD peak deconvolution (Figure 2) shows the peak corresponding to GaN with wurtzite structure along the (0002) plane at 34.58° (Pattern: 00-050-0792) [10]. The peak at 34.2° comes from InN (111) (Pattern: 01-070-2563) and the peak corresponding to $In_xGa_{1-x}N$ (0002) is located at 33.55° [2, 11]. The other diffraction peak founding in the diffractograms correspond to the In (101) incorporation at 32.9° (Pattern: 00-005-0642) [12]. The XRD peak deconvolution for sample B (Figure 3) shows the diffraction peaks for GaN (0002), InN (111) and $In_xGa_{1-x}N$ (0002) at 34.58°, 34.0° and 33.56°, respectively. With the change in the growth pressure, sample B, the peak related to metallic indium tend to disappear. This indicates that the alloy formation is favored at high pressures (550 Torr) near to atmospheric pressure.

Lattice parameter determination provides information on both composition and residual strain of the films. Assuming the epitaxial film to be fully relaxed, the lattice parameter is only affected by the chemical composition. The lattice constants in the growth direction, *c*(GaN) and *c*(InGaN), for any allowed (00.*l*) reflection, are given directly by Bragg's law [13]:

$$c = \frac{l\lambda}{2sin\theta} \qquad (1)$$

Using radiation of wavelength λ = 1.5406 Å and with the relevant Bragg angle (θ_B), estimated from the XRD distribution peak. The sample A lattice constants obtained by use of Eq. (1) are *c*(GaN) = 5.183 Å and *c*(InGaN) = 5.343 Å. For the sample B, lattice constants obtained are *c*(GaN) = 5.185 Å and *c*(InGaN) = 5.335 Å.

According to the Vegard's law, a ternary alloy shows a linear dependence of lattice parameter on composition, therefore, the indium composition (*x*) can be derived from the plane spacing measured in one specific direction. This is obtained from the out-of-plane lattice parameter *c* of alloy film, by the following expression [14]:

$$c(x) = c_0^{GaN}(1-x) + c_0^{InN}x \qquad (2)$$

where c_0^{GaN} = 5.1850 Å, c_0^{InN} = 5.7033Å. Then, the compositions obtained from Eq. (2) were x_A= 0.304 and x_B = 0.289. It can be expressed as $In_{0.3}Ga_{0.7}N$ for sample A, and $In_{0.29}Ga_{0.71}N$ for sample B. These values were used for calculate the lattice constant *a*(InGaN) for both samples by the following equation:

$$a(x) = a_0^{GaN}(1-x) + a_0^{InN}x \qquad (3)$$

where $a_0^{GaN} = 3.1892\,\AA$, and $a_0^{InN} = 3.5378\,\AA$. The respective lattice constants obtained are $a(InGaN)_A$ = 3.2938 Å and $a(InGaN)_B$ = 3.2899 Å.

The energy gap width is determined as a function of the local composition of the $In_xGa_{1-x}N$ solid solution by the expression [15 - 17]:

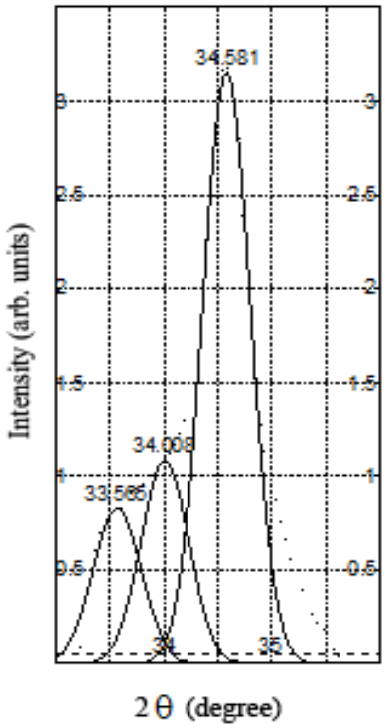

Figure 3. Deconvolution of X-ray diffraction pattern for $In_xGa_{1-x}N$ layer (sample B). The peaks at 34.58° and 33.56° represent the (0002) diffraction peaks of GaN with wurtzite structure and $In_xGa_{1-x}N$ (0002) diffraction peak, respectively. The peak located at 34° corresponds to InN (111) diffraction peak.

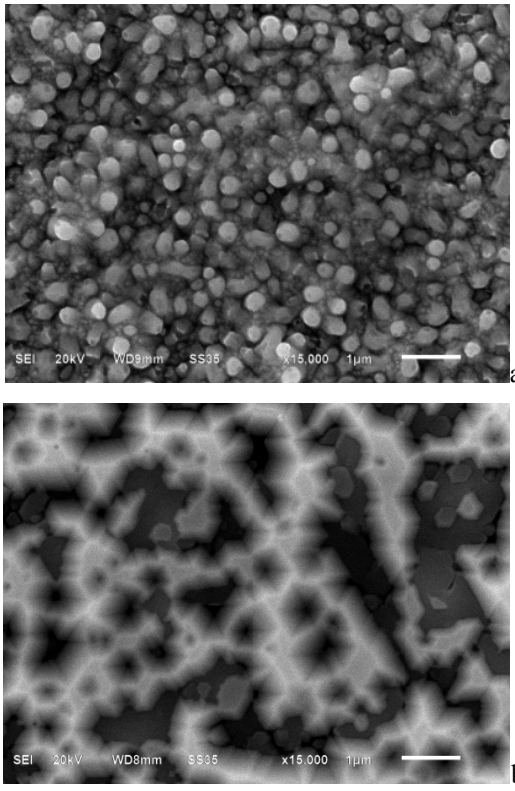

Figure 4. SEM images of (A) $In_{0.3}Ga_{0.7}N$ and (B) $In_{0.29}Ga_{0.71}N$ grown at 50 and 550 Torr, respectively.

(4)

Where E^{GaN} = 3.4 eV, E^{InN} = 0.7 eV, and b = 1.43 eV is the approximation parameter [18, 19]. The energies gap calculated are $E_g(In_{0.3}Ga_{0.7}N)$ = 2.28 eV and $E_g(In_{0.29}Ga_{0.71}N)$ = 2.3 eV.

Scanning electron microscopy (SEM) was done using a Scanning Electrón Microscope Jeol JSM 6610LV, the applied voltage was 20 kV. SEM images shown in Figure 4(A) and 4(B) illustrate the effect of the growth pressure on the films surface morphology. Sample A (50 Torr) has a smaller grain size and higher nuclei density. As the pressure is increased to 550 Torr the surface of the sample B is composed of the planar regions and by hexagonal three dimensional (3D) islands. The island size increases and has lower density, because the adatom migration decreases at high pressure. Also, the adatom migration is usually suppressed at low temperatures; the decreased mobility of surface species promotes a uniform dispersion of nuclei that can effectively cover the substrate [20].

4. Conclusions

$In_xGa_{1-x}N$ layers growth on GaN templates by a MOCVD system were investigated at 50 y 550 Torr. Both samples have face separation. The sample growth at low pressure has the InN, InGaN and In faces. The sample growth at high pressure shows better morphological and structural characteristics, because there is no indium incorporation as metal and no droplets were formed on the surface, it is observed the island growth with hexagonal form. Also, the diffraction peak corresponding to the InN face show lower intensity compared to the diffraction peak corresponding to the InGaN face. Therefore, not only the low temperatures favor the formation of the alloy, the high pressures allow bigger indium incorporation in the GaN crystal structure too.

Acknowledgements

The authors want to acknowledgements Tec. D. Ramirez (SEES-CINVESTAV) for his technical assistance, Dr. A. Escobosa (SEES-CINVESTAV) for his support in X-ray diffraction, Dr. E. Rubio and R. Agustin (CUV-BUAP) for his support in SEM images acquisition.

References

[1] N. A. El-Masry, E. L. Piner, S. X. Liu, S. M. Bedair, Phase separation in InGaN grown by metalorganic chemical vapor Deposition, Applied Physics Letters **72** (1998) 40.

[2] X. L. Zhu, L. W. Guo, B. H. Ge, M. Z. Peng, N. S. Yu, J. F. Yan, J. Zhang, H. Q. Jia, H. Chen, and J. M. Zhou, Observation of metallic indium clusters in thick InGaN layer grown by metal organic chemical vapor deposition, Applied Physics Letters **91** (2007) 172110.

[3] A. Krost, and J. Bla Sing, H. Protzmann, M. Lunenburger, and M. Heuken, Indium nanowires in thick (InGaN) layers as

determined by x-ray analysis, Applied Physics Letters **76** (2000) 1395.

[4] Victor-Tapio Rangel-Kuoppa, Cesia Guarneros Aguilar, Victor Sánchez-Reséndiz, Structural, optical and electrical study of undoped GaN layers obtained by metalorganic chemical vapor deposition on sapphire substrates, Thin Solid Films **519** (2011) 2255.

[5] C. Guarneros, V. Sanchez, GaN buffer layer growth by MOCVD using a thermodynamic non- equilibrium model, Vacuum **84** (2010) 1187.

[6] P. Ruterana, G. Nouet, W. Van der Stricht, I. Moerman, and L. Considine, Chemical ordering in wurtzite $In_xGa_{1-x}N$ layers grown on (0001) sapphire by metalorganic vapor phase epitaxy, Applied Physics Letters **72** (1998) 1742.

[7] D. Doppalapudi, S.N. Basu, K.F. Ludwing, and T.D. Moustakas, Phase separation and ordering in InGaN alloys grown by molecular beam epitaxy, Journal of Applied Physics **84** (1998) 1389.

[8] D. Doppalapudi, S.N. Basu, and T.D. Moustakas, Domain structure in chemically ordered $In_xGa_{1-x}N$ alloys grown by molecular beam epitaxy, Journal of Applied Physics **85** (1999) 883.

[9] M.K. Behbehani, E.L.Piner, S.X. Liu, N.A. El-Masry, and S.M. Bedair, Phase separation and ordering coexisting in $In_xGa_{1-x}N$ grown by metal organic chemical vapor deposition, Applied Physics Letters **75** (1999) 2202.

[10] B. Shen, Y. G. Zhou, Z. Z. Chen, P. Chen, R. Zhang, Y. Shi, Growth of wurtzite GaN films on a-Al_2O_3 substrates using light-radiation heating metal-organic chemical vapor deposition, Journal of Applied Physics A **68** (1999) 593.

[11] O. Jani, C. Honsberg, Y. Huang, J-O Song, I. Ferguson, G. Namkoong, E. Trybus, A. Doolittle, S. Kurtz; Design, Growth, Fabrication and Characterization of High-Band GaP InGaN/GaN Solar Cells, Conference Record of the 2006 IEEE 4th World Conference on Photovoltaic Energy Conversion (IEEE,New York, 2006), V. 1 p. 20.

[12] B. N. Pantha, J. Li, J. Y. Lin, H. X. Jiang, Single phase $In_xGa_{1-x}N$ ($0.25 \leq x \leq 0.63$) alloys synthesized by metal organic chemical vapor deposition, Applied Physics Letters **93** (2008) 182107.

[13] K. P. O'Donnell, J. F.W. Mosselmans, R. W. Martin, S. Pereira and M. E. White, Structural analysis of InGaN epilayers, Journal of Physics: Condensed Matter **13** (2001) 6977.

[14] G. Xi, W. Hui, J. De-Sheng, W. Yu-Tian, Z. De-Gang, Z. Jian-Jun, L. Zong-Shun, Z. Shu-Ming, and Y. Hui, Evaluation of both composition and strain distributions in InGaN epitaxial film using x-ray diffraction techniques, Chinese Physic B **19** (2010) 106802.

[15] M. Kurouchi, T. Araki, H. Naoi, T. Yamaguchi, A. Suzuki, and Y. Nanishi, Growth and properties of In-rich InGaN films grown on (0001) sapphire by RF-MBE, Physica Status Solidi (b) **241** (2004) 2843.

[16] H. J. Kim, Y. Shin, Soon-Yong Kwon, H. J. Kim, S. Choi, S. Hong, C. S. Kim, Jung-Won Yoon, H. Cheong, E. Yoon, Compositional analysis of In-rich InGaN layers grown on GaN templates by metalorganic chemical vapor deposition, Journal of Crystal Growth **310** (2008) 3004.

[17] Yen-Kuang Kuo, Bo-Ting Liou, Sheng-Horng Yen, Han-Yi Chu, Vegard's law deviation in lattice constant and band gap bowing parameter of zincblende $In_{1-x}Ga_xN$, Optics Communications **237** (2004) 363.

[18] J. Wu, W. Walukiewicz, K. M. Yu, and J. W. Ager III, E. E. Haller, Hai Lu and William J. Schaff, Small band gap bowing in $In_{1-x}Ga_xN$ alloys, Applied Physics Letters **80** (2002) 4741.

[19] C. Caetano, L.K. Teles, M. Marques, A. Dal Pino Jr., L.G. Ferreira, Phase stability, chemical bonds, and gap bowing of $In_{1-x}Ga_xN$ alloys: Comparison between cubic and wurtzite structures, Physical Review B **74** (2006) 045215.

[20] N. K. van der Laak, R. A. Oliver, M. J. Kappers, C. McAleese and C. J. Humphreys, Stranski-Krastanov growth for InGaN/GaN: wetting layer thickness changes, Microscopy of Semiconducting Materials: Microscopy of Semiconducting Materials: Springer Proceedings in Physics **107** (2005) 13